Enthalpic and Entropic Components of Cooperativity for the Partially Ligated Intermediates of Hemoglobin Support a "Symmetry Rule" Mechanism†

Yingwen Huang and Gary K. Ackers*

Department of Biochemistry and Molecular Biophysics, Washington University School of Medicine, St. Louis, Missouri 63110

Received November 22, 1994; Revised Manuscript Received January 26, 1995®

ABSTRACT: Subunit assembly reactions of hemoglobin's 10 ligation microstates have been studied as a function of temperature to evaluate the enthalpic and entropic components of cooperativity. It is found that the cooperative enthalpies and cooperative entropies distribute in close agreement with predictions of the symmetry rule mechanism (Ackers et al., 1992) previously deduced from the free energy distribution, in combination with structure-sensitive probes (Doyle & Ackers, 1992; LiCata et al., 1993; Daugherty et al., 1994). Principal findings of the present study are as follows: (1) In unligated hemoglobin (quaternary T), dimer−tetramer assembly is driven by a large negative enthalpy, whereas in the fully ligated (quaternary R) species, the driving force for quaternary assembly is entropic. For the eight intermediate ligation species, the switchover from enthalpic to entropic control follows precisely the symmetry rule predictions; i.e., switching from enthalpic to entropic control occurs at each of the six steps that create ligated heme sites on both sides of the dimer−dimer interface. The combinatorial distribution found previously with free energies does not therefore arise from coincidental enthalpy−entropy compensation that masks a more fundamental distribution. (2) The free energy of tertiary constraint ΔG_{tc}, which pays for intradimer cooperativity prior to quaternary switching, contains large enthalpic and entropic components ΔH_{tc} and ΔS_{tc}. Like ΔG_{tc}, these terms vanish at the second binding step within the T tetramer. It is found that ΔG_{tc} arises from a net enthalpic dominance over an almost equally large $T\Delta S_{tc}$. (3) The stepwise enthalpies correlate with stepwise values of Bohr protons and Bohr free energies (Daugherty et al., 1994) throughout the cascade of 16 stepwise reactions; the correlated clusters of these values follow predictions of the symmetry rule mechanism. (4) These results obtained with cyanomethemoglobin are consistent with the corresponding data on oxygenated hemoglobin which has been resolved at each stage of oxygenation.

A central goal in hemoglobin (Hb) research has been to resolve the molecular processes that give rise to cooperativity[1] as reflected in the sigmoidal shape of the binding isotherm:

$$\bar{Y} = \frac{\sum_{i=0}^{4} iK_{4i}[X]^i}{4\sum_{i=0}^{4} K_{4i}[X]^i} \quad (1)$$

where $\bar{Y}$ is the fraction of heme sites occupied by the bound ligand species X (e.g., O_2, CO, NO, CN) at concentration [X]. Each Adair binding constant K_{4i} reflects the free energy of reacting i sites ($i = 1-4$; $K_{40} = 1$). Alternatively, the sequential stages of binding (i.e., where changes in number of ligands bound are $0 \rightarrow 1$, $1 \rightarrow 2$, $2 \rightarrow 3$, and $3 \rightarrow 4$) can be described by the "stagewise" binding constants, k_{4i}:

$$k_{4i} = \frac{K_{4i}}{K_{4(i-1)}} \quad (2)$$

Variation of k_{4i} values with the number i of ligands bound (per mole of Hb) leads to binding curves that deviate from the hyperbolic (noncooperative) shape.[2] If the successive values of k_{4i} increase (after correction for statistical factors), it means that early binding enhances the Hb molecule's affinity for subsequent binding at the remaining sites. Such cooperativity, arising from ligand-induced structural changes of the Hb molecule, must be "paid for" by equivalent free energy of structural alteration in order to maintain energy balance. The ligand-induced structural changes are classified as "quaternary" (i.e., T → R rearrangement of dimeric half-molecules)[3] or "tertiary" (i.e., ligand-driven conformational transitions which occur additionally to the quaternary T → R shifts). Much work has pointed to the importance of coupling between the tertiary and quaternary transitions as a major determinant of the cooperative mechanism. For example, the classical allosteric mechanisms (Monod et al., 1965; Koshland et al., 1966) differ principally through their

† This work was supported by NSF Grant DMB9107244 and NIH Grants R37-GM24486 and HL51084.

* To whom correspondence should be addressed.

® Abstract published in *Advance ACS Abstracts,* March 15, 1995.

[1] A major physiological significance of the cooperative (sigmoidal) shape is to permit efficient delivery of oxygen to the tissues.

[2] The Hill coefficient (a traditional index reflecting overall cooperativity) is calculated as $n_H = \{d \ln [\bar{Y}/(1 - \bar{Y})]\}/d \ln [x]$, where $[x]$ is the concentration of unbound heme site ligand. n_H measures cooperativity by reflecting statistical variance in the distribution of i-ligated species (Edsall & Gutfreund, 1978). As such it provides no determination of the distribution itself nor of individual microstate properties.

[3] All reference to "quaternary structural transition" here will denote the global (T to R) reorientation of the $\alpha\beta$ dimers which accompanies complete heme site ligation as determined from crystal structure analysis (Baldwin & Chothia, 1979). Recent crystallographic work (Smith et al., 1990; Silva et al., 1992; Smith & Simmons, 1994) has demonstrated a third quaternary structure ("quaternary Y") which is accessible to fully ligated hemoglobin. Conclusions of the present work would not be altered whether the fully ligated cyanomet tetramers are in quaternary Y or in quaternary R.

0006-2960/95/0434-6316$09.00/0

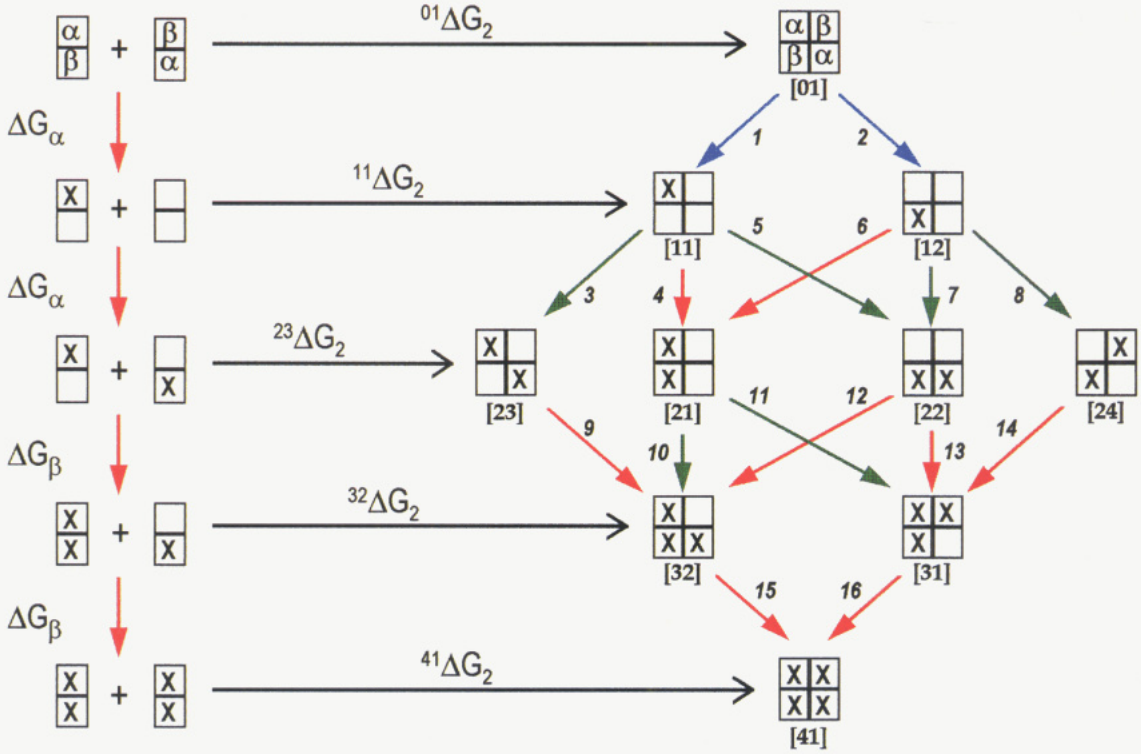

FIGURE 1: Cascade of stepwise ligation reactions for hemoglobin tetramers (right) in linkage with constituent dimers (left). The linked dimer to tetramer assembly reactions are used to measure the energetic costs of tetrameric cooperativity for the various steps (see text). Molecular species are depicted topographically with dimers assembling to form the $\alpha^1\beta^2$ interface (vertically bisecting each tetramer). Relative orientation of subunits within the tetramers is indicated in the top species [01]. Index [*ij*] denotes the particular species *j* among those with *i* ligands bound ($i = 0-4$, $j = 0-4$). Ordering of species with respect to *j* is arbitrary. Ligated heme site (×) in this study contains Fe(III)-CN, while Fe(II) is in each unligated (blank) subunit. Arrow colors denote tertiary constraint transitions (blue), switchpoint transitions (green), and null transitions (red), as quantified in Table 2.

divergent approaches to these couplings. To develop an appropriate experimental framework for addressing the structural issues of ligand-driven tertiary vs quaternary transitions, the energetics of cooperativity must be analyzed at a level of detail which takes into account the configurational isomers for each number *i* of ligands bound[2] (see Figure 1). This imperative was validated by the discovery that cooperative free energy transduction can depend strongly on the configuration of ligated and unligated sites within the tetrameric structure (Smith & Ackers, 1985).

Using Assembly to Measure Energetic Binding Penalties. Thermodynamic linkage relationships between tetramers and their dissociated dimers ($\alpha\beta$) (Ackers & Halvorson, 1974) have been used extensively to evaluate the stagewise free energy costs of cooperativity for oxygen binding (Mills et al., 1976; Atha et al., 1979; Mills & Ackers, 1979; Chu et al., 1984; Ackers & Johnson, 1990; Doyle et al., 1991, 1992). The dissociated dimers provide an especially useful set of reference species since their oxygen binding reactions occur noncooperatively and with the same affinity as the isolated subunits. Extension of these oxygen binding techniques to the nine microstate ligation species (Figure 1) has not been possible due to extreme lability of O_2 at the sites and the tendency for partially ligated tetramers to dissociate and reassemble into mixed-site configurations. However, a strategy that has proved uniquely successful in resolving cooperativities for all nine Hb ligation species (Figure 1) is based on determining the stepwise "free energy penalties", i.e., the energy by which each binding to a site (or combination of sites) within the tetramer deviates from that of a noncooperative reference reaction of the same sites. Each penalty is evaluated as the difference between the energy of binding *i* ligands onto the tetrameric sites and binding onto the same site(s) within dimers. These penalties have been evaluated by measuring the linked energetics of subunit assembly for all 10 ligation species shown in Figure 1 using analogs of oxygenated heme sites [e.g., CN, CO, Mn(III)] and of deoxygenated heme sites [Fe(II), Co(II)]. In these systems, cooperativity of heme site ligation has been resolved in detail by measuring the free energies of assembly for both "reactant" and "product" species in all 16 steps of the cascade (Ackers et al., 1992; Doyle & Ackers, 1992).

The approach is illustrated by considering the linked assembly reactions for the five leftmost tetramers, i.e., connected by stepwise ligation reactions 1, 3, 9, and 15. By virtue of the path independence of ΔG we may write the following expressions of free energy balance:

$$\Delta G_1 = \Delta G_\alpha + (^{11}\Delta G_2 - {}^{01}\Delta G_2) \quad (3a)$$

$$\Delta G_{(1+3)} = 2\Delta G_\alpha + (^{23}\Delta G_2 - {}^{01}\Delta G_2) \quad (3b)$$

$$\Delta G_{(1+3+9)} = 2\Delta G_\alpha + \Delta G_\beta + (^{32}\Delta G_2 - {}^{01}\Delta G_2) \quad (3c)$$

$$\Delta G_{(1+3+9+15)} = 2(\Delta G_\alpha + \Delta G_\beta) + (^{41}\Delta G_2 - {}^{01}\Delta G_2) \quad (3d)$$

On the left of each equation is the standard Gibbs energy for the sequence of stepwise reactions indicated in subscript (reactions are taken from left to right and top to bottom). On the right are binding free energies for the α or β sites of the dissociated dimer (ΔG_α, ΔG_β) plus the difference between assembly energies of species *ij* and 01. This difference ($^{ij}\Delta G_2 - {}^{01}\Delta G_2$), which is termed the "cooperative free

energy" (symbolized by ${}^{ij}\Delta G_c$), measures the energetic cost of binding i heme site ligands to form species ij (i.e., the excess energy over that of binding the same sites as dimers). For example, eq 3d can be written

$$\sum \Delta G_{steps} - 2(\Delta G_\alpha + \Delta G_\beta) = {}^{41}\Delta G_c \qquad (3e)$$

where ${}^{41}\Delta G_c$ is the overall "cooperative free energy", comprising the sum of energy costs for complete ligation along any path of Figure 1 (e.g., reactions 2 + 6 + 11 + 16). Experimental determination of the two assembly energies ${}^{41}\Delta G_2$ and ${}^{01}\Delta G_2$ thus provides an exact measure of the difference between the binding free energy of tetramer and that of the corresponding sites within dissociated (noncooperative) dimers.

A similar relation to eq 3e also applies to any of the subcycles represented by eqs 3a, 3b, or 3c. For example, eq 3b "encompasses" the subcycle of eq 3a so that the "free energy distance" between species [23] and [11] (i.e., reaction 3) is calculated from (3b) − (3a): $\Delta G_3 = \Delta G_\alpha + ({}^{23}\Delta G_2 - {}^{11}\Delta G_2)$. The rightmost term here is the cooperative free energy of binding to the second α subunit within a tetrameric structure, given that the first α subunit has already been occupied. Partitioning of the total cooperative free energy ${}^{41}\Delta G_c$ among stepwise reactions in the cascade (Figure 1) is thus obtained by taking differences between their respective ${}^{ij}\Delta G_c$ values.[4] Corresponding relationships which apply to other state functions (e.g., ΔH, ΔS) will be discussed in subsequent sections.

Early applications of this approach to the cyanomet ligation system (Smith & Ackers, 1985; Perrella et al., 1990) found that the 10 microstates distribute with just three values of cooperative free energy and that the doubly ligated species segregate in a combinatorial fashion into two separate levels (Figure 2); i.e., species [21] has the same cooperative free energy as the two singly ligated molecules but species [22], [23], and [24] occupy the third level along with species [31], [32], and [41]. This tripartite distribution was also found in the Fe(II)/Mn(III) system[5] (Smith et al., 1987; Ackers, 1990). Additional studies have revealed that this ligation system and the cyanomet system represent simplified cases of a slightly more complex five-level energetic distribution which is exemplified by the Co(II)/Fe(II)CO system[5] (Speros et al., 1991; Doyle et al., 1991). A common feature of all these explicitly resolved systems is that the four doubly ligated tetramers distribute into two cooperative free energies. This finding alone precludes the MWC model of allosteric control [Monod et al., 1965; cf. Ackers (1990)].

[4] These free energy parameters can be explicitly related to the Adair binding constants of eq 1, starting from a general form of eq 3e, $K'_{ij} = (K_\alpha)^p(K_\beta)^q \exp(-{}^{ij}\Delta G_c/RT)$, where K'_{ij} is the equilibrium constant for formation of species ij from species 01 and i ligands, p and q are the respective numbers of α and β hemes ligated, and K_α and K_β are their site binding constants on dimers (Figure 1). Then each Adair constant of eq 1 may be written $K_{4i} = \sum_{\{ij\}} g_{ij}(K_\alpha)^p(K_\beta)^q \exp(-{}^{ij}\Delta G_c/RT)$, where g_{ij} is the statistical degeneracy of species ij (see legend to Figure 1). The sum is over all configurational isomers ij that have i sites bound (Figure 1). From this relationship we can write the tetrameric binding partition function, $X = \sum_{i=0}^{4} K_{4i}(x)^i = \sum_{i=0}^{4}(x)^i \sum_{\{ij\}} g_{ij}(K_\alpha)^p(K_\beta)^q \exp(-{}^{ij}\Delta G_c/RT)$. The tetrameric binding isotherm $\bar{Y}$ is directly calculable from this partition function by the standard relationship [cf. Hill (1960)]: $\bar{Y} = {}^1/_4 \partial \ln X/\partial \ln [x]$.

[5] Ligation systems are designated by the form M(n)L/M′(n')L′, where symbols left and right of the slash denote the unligated sites and ligated sites, respectively; M and M′ are heme metals, n and n' are their oxidation states, and L and L′ are the bonded ligands.

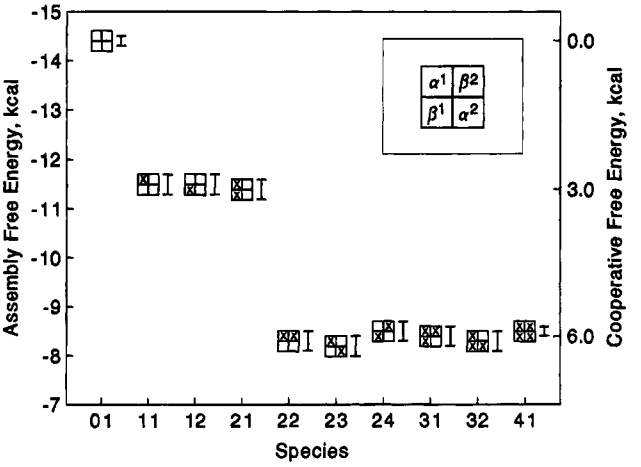

FIGURE 2: Distribution of cooperative free energies for the 10 ligation microstates of cyanomethemoglobin. Conditions are 0.1 M Tris-HCl, 0.1 M NaCl, and 1 mM Na_2EDTA, pH 7.4, 21.5 °C.

Table 1: Phased Distribution of Cooperative Free Energy through the Cascade of Heme Site Binding[a]

binding reaction	stepwise ΔG_c^s	synchronized switches[b]	mean response
1	3.0 ± 0.2	tc	3.15 ± 0.3
2	3.3 ± 0.2		
4	0.1 ± 0.3	null	−0.1 ± 0.3
6	−0.2 ± 0.3		
9	−0.2 ± 0.3		
12	−0.2 ± 0.3		
13	0.0 ± 0.3		
14	−0.1 ± 0.3		
15	−0.1 ± 0.3		
16	−0.3 ± 0.3		
3	2.9 ± 0.3	sw	3.1 ± 0.3
5	3.3 ± 0.3		
7	3.0 ± 0.3		
8	3.1 ± 0.3		
10	3.0 ± 0.3		
11	3.2 ± 0.3		
net overall cooperative energy			6.1 ± 0.3

overall switches[c]	free energy penalty	transition	mean response
01 → 22	6.3 ± 0.3	T→R	6.2 ± 0.3
01 → 23	5.9 ± 0.3		
01 → 24	6.4 ± 0.3		
01 → 31	6.3 ± 0.3		
01 → 32	6.1 ± 0.3		
01 → 41[d]	6.0 ± 0.3		

[a] See Figure 1. Ligated heme sites are Fe(III)-CN. [b] Ligation-driven transitions for generation of tertiary constraint (tc); release of tertiary constraint plus T → R quaternary switching (sw); no free energy increment over that of dissociated dimers (null). [c] Free energy penalty for ligation up to the points where both dimeric half-molecules contain ligated heme sites. [d] Complete ligation of all sites (by any pathway through the cascade).

The following were seen from the early results on cyanomet ligation (e.g. Table 1, Figure 2): (a) A free energy penalty (i.e., 3 kcal at pH 7.4, 21.5 °C) is paid for the first binding step onto the tetramer (i.e., reactions 1 or 2 of Figure 1). (b) Binding a second ligand onto the same dimeric half-tetramer (i.e., reactions 4 and 6) occurs with no additional penalty and thus is 3 kcal more favorable than binding to the first site; affinity of the second binding step is identical to that of the dissociated dimer but is 170-fold more favorable than the first binding step. (c) An additional penalty (also 3 kcal at pH 7.4) is "paid" at each of the six binding steps which create tetramers with ligands on both dimeric halves

(i.e., reactions 3, 5, 7, 8, 10, and 11). (d) In addition to reactions 4 and 6, there are six other stepwise reactions that are unaccompanied by energetic penalties (i.e., reactions 9, 12, 13, 14, 15, and 16). This extreme specificity in pathways of cooperative energy flow that was revealed by the initial study (Smith & Ackers, 1985) has provided impetus for work on this problem over the last decade. Our goals have been to delinate the coupling rules for ligand-driven quaternary and tertiary structural transitions within the cascade of 16 heme site binding steps and to understand their relationship to structural features and mechanisms of control by heterotropic effectors (protons, chloride, DPG, CO_2).

Symmetry Rule. Properties of the 10 ligation species have been correlated with a variety of structure-sensitive probes (Daugherty et al., 1991, 1994; Ackers et al., 1992; Doyle & Ackers, 1992; LiCata et al., 1993). In combination with the energetics of cooperativity mentioned above, these studies led to the proposal of a symmetry rule for distribution of the 10 ligation species among the two quaternary structures: *switching from quaternary T to quaternary R occurs when a tetramer acquires at least one ligand bound on each dimeric half-molecule, i.e.,* $\alpha^1\beta^1$ *and* $\alpha^2\beta^2$. The symmetry rule thus defines specific conditions on heme site ligation that lead to the quaternary T → R transitions. It translates the 10 combinatorial forms of ligated and unligated sites into six T → R switch points. The same studies have indicated the intermediate "allosteric state" (species [11], [12], and [21]) to have the quaternary T interface [cf. LiCata et al. (1993)].

Mechanism of Cooperativity. From results mentioned above, the following picture has emerged regarding transduction of heme site binding energy into the tertiary and quaternary structural transitions.

(1) Binding an initial ligand onto the tetramer induces alterations that affect net binding energy at both sites within the dimeric half-molecule to which the ligand is bound. A positive free energy penalty ΔG_{tc} is generated which opposes the larger (negative) "intrinsic" free energy of binding. Since species [11], [12], and [21] have the quaternary T structure, ΔG_{tc} reflects ligand-induced conformational work performed against the quaternary T interface, which serves as a mechanical constraint. This "tertiary constraint" effect simultaneously involves both α and β subunits within the half-molecule. Binding the first ligand (either to α or to β) increases the affinity for ligating the other subunit. Hemoglobin thus exhibits cooperative binding within its quaternary T structure.

(2) Generation of tertiary constraint energy ΔG_{tc}, which pays for intradimer cooperativity within T, occurs without breaking local bonds of the dimer−dimer interface. This conclusion arises from extensive single-residue mutational studies of energetic perturbations to the dimer−dimer interface in species [01], [21], and [41] (LiCata et al., 1993): (a) ΔG_{tc} is not affected by mutationally altering residues of the adjacent dimer. If ligating the T tetramer of normal Hb were to break interfacial bonds with energy of breakage ΔG_{tc} (or a significant fraction thereof), then the value of ΔG_{tc} should be different when the "acceptor residues" on the adjacent (unligated) dimer were modified to preclude bond formation. (b) However, it was found that the modifications of these interfacial residues on one dimer and heme site ligation of the adjacent dimer are energetically independent (LiCata et al., 1993). The contribution of ΔG_{tc} from ligand-induced breakage of noncovalent bonds associated with those residues was evaluated to be less than 0.3 kcal/residue (LiCata et al., 1993).

(3) Within a quaternary T tetramer only one of the dimers can manifest tertiary constraint. The T interface cannot accommodate two such perturbed dimers: an additional energy penalty for binding to the second dimer within T causes the R interface to be favored by molecules which are ligated on both dimers (Ackers et al., 1992).

(4) Quaternary T to R switching releases the previously stored ΔG_{tc} and also breaks the noncovalent bonds (including salt bridges) at the interface. A new dimer−dimer interface (quaternary R or Y) is formed with a less favorable free energy so that the net energetic effect is positive. Since the energy of T → R transition is larger (i.e., more positive) than ΔG_{tc}, the system experiences an increment of cooperative free energy equal to $\Delta G_{T\rightarrow R} - \Delta G_{tc}$ at each of the six switch points specified by the symmetry rule. The cooperative energy-generating effects of tertiary constraint and quaternary switching are thus distributed through the cascade of binding pathways. The symmetry rule mechanism predicts that a functional response F which is driven by heme site ligation will be manifested at each of the six switch point transitions by the values of three characteristic parameters according to the relationship

$$F_{sw} = F_{T\rightarrow R} - F_{tc} \quad (4)$$

A specific synchronization and phasing of the response functions through designated subsets of the 16 transitions is thus predicted. In addition to the two tertiary constraint-generating reactions (tc) and the six switch point transitions (sw), the mechanism predicts eight reactions where response is identical to that of dissociated dimers ("null"). The synchronized sets of cooperative ΔG transitions are shown in Table 1 for the cyanomet system at pH 7.4, 21.5 °C.

(5) Additional cooperativity can arise as a result of "quaternary enhancement", i.e., affinity at the last binding steps may exceed that of the intrinsic (dimer) value (Mills & Ackers, 1979; Ackers & Johnson, 1990; Doyle et al., 1991; Doyle & Ackers, 1992).

Coupling to Bohr Protons. Heterotropic responses of the hemoglobin mechanism were recently analyzed for the linked processes of proton binding, heme site ligation, and quaternary assembly (Daugherty et al., 1994). It was found that the 16 ligation steps of cyanomethemoglobin exhibit two distinct Bohr effects which distribute in accord with predictions of the symmetry rule: A "tertiary Bohr effect" arises from initial ligation within the T tetramer (reactions 1 and 2 of Figure 1) and is correlated with the generation of ΔG_{tc}. The second Bohr effect occurs at each of the six switch point transitions (sw) which are specified by the symmetry rule (i.e., at reactions 3, 5, 7, 8, 10, and 11 of Figure 1). In these transitions tertiary constraint is released, the quaternary T interface breaks, and the R interface is formed. The net release of Bohr protons at each switch point is thus a difference between the quaternary (T → R) Bohr protons and the tertiary Bohr protons. An especially striking feature was that the eight "null transitions" (i.e., 4, 6, 9, 12, 13, 14, 15, and 16) where heme site binding is unaccompanied by expenditure of cooperative free energy (ΔG_c) also showed no proton linkages; i.e., at these transitions, tetrameric binding affinity and Bohr effects are quantitatively identical to those of dissociated dimers (see Table 2). These results were also consistent with measured proton release that

Table 2: Synchronized Clusters of Response Parameters for Cyanomethemoglobin, pH 7.4[a]

	stepwise parameter	tertiary constraint transitions (1,2)	null transitions (4,6,9,12,13,14,15,16)	switch point transitions (3,5,7,8,10,11)	overall transitions (T→R)
1	ΔG_c^s	3.2 ± 0.2	−0.1 ± 0.3	3.1 ± 0.3	6.2 ± 0.3
2	ΔG_c^s	3.3 ± 0.3	0.0 ± 0.2	3.4 ± 0.4	6.7 ± 0.5
3	ΔG_{Bohr}^s	0.7 ± 0.2	0.0 ± 0.2	2.3 ± 0.2	3.0 ± 0.3
4	$\Delta \nu_c^s$	0.7 ± 0.2	0.0 ± 0.2	0.8 ± 0.2	1.5 ± 0.3
5	ΔH_c^s	14 ± 3	1 ± 3	14 ± 3	29 ± 3
6	$-T\Delta S_c^s$	−11 ± 3	−1 ± 3	−11 ± 3	−23 ± 3

[a] (1) Cooperative free energies obtained with cyanomet as sole ligand (Smith & Ackers, 1985; Perrella et al., 1990; this study). (2) From free energies of binding oxygen onto the vacant sites of partially ligated cyanomet species (Doyle & Ackers, 1992). (3) Bohr proton-linked free energies (Daugherty et al., 1994). (4) Number of Bohr protons released (Daugherty et al., 1994). (5) Cooperative enthalpies (this study; see Table 3). (6) Cooperative entropy contributions (this study; see Table 3). Clusters are denoted by arrow colors of Figure 1.

accompanies oxygenation of vacant sites on the cyanomet microstates (Perrella et al., 1994).

Enthalpic and Entropic Components. In the present study we have carried out experiments to assess the detailed enthalpic and entropic components of the cooperative free energies in order to explore further the nature and origins of symmetry rule behavior. Is the dramatic synchronization and phasing of cooperative free energies and Bohr protons which occurs through specific subsets of the 16 transitions also manifested by the enthalpy- and entropy-generating processes which accompany heme site ligation? Or does the distribution of $^{ij}\Delta G_c$ values conform to predictions of the symmetry rule mechanism solely as a result of enthalpy−entropy compensation? Is the observed tertiary constraint effect predominantly enthalpic or entropic? The same questions arise for the quaternary T → R free energy. An additional concern is how the enthalpic and entropic responses induced by heme site ligation may be related to the molecule's interactions with heterotropic regulators such as H^+, i.e., to the "tertiary", "quaternary", and "null" Bohr effects.

To address these issues we have employed the same linkage strategy that was used to analyze cooperative free energies (Figure 1). Thus, we consider the corresponding enthalpic and entropic relationships:

$$^{ij}\Delta H_c = {}^{ij}\Delta H_2 - {}^{01}\Delta H_2 = \Delta H_{ij} - (p\Delta H_\alpha + q\Delta H_\beta) \quad (5)$$

$$^{ij}\Delta S_c = {}^{ij}\Delta S_2 - {}^{01}\Delta S_2 = \Delta S_{ij} - (p\Delta S_\alpha + q\Delta S_\beta) \quad (6)$$

where subscripts and superscripts correspond with free energies already discussed: $^{ij}\Delta H_c$ is cooperative enthalpy as measured by the assembly enthalpies $^{ij}\Delta H_2$ (eq 5) and equals the difference between binding heat for tetrameric ligation ΔH_{ij} and that of the constituent sites (ΔH_α and ΔH_β) binding as dissociated dimers. Corresponding definitions apply to the entropies of eq 6.

MATERIALS AND METHODS

All experiments were carried out in standard buffer consisting of 0.1 M Tris-HCl, 1 mM Na_2EDTA, 10 μM KCN, and 0.18 M NaCl. The standard buffer was titrated with HCl to pH 7.40 ± 0.01 at the temperature of each experiment. The exact amount of sodium chloride added was calculated at each temperature to give a final concentration of 0.18 M total chloride. Trizma base, Na_2EDTA, and NaCl were from Sigma. Potassium ferricyanide and KCN were from VWR Scientific. Phosphate-free hemoglobin A_0 was prepared by the method of Williams and Tsay (1973). Fully cyanomethemoglobin A_0 was prepared as described (Smith & Ackers, 1985). Hemoglobin species [23] and [24] were prepared by using a modified version of the method of Blough and Hoffman (1984).

Dimer−Tetramer Assembly by Anaerobic Gel-Permeation Chromatography. Assembly equilibria for doubly ligated cyanomet species [23] and [24] and fully ligated species [41] were measured anaerobically by analytical gel chromatography (Ackers, 1970; Valdes & Ackers, 1979) using Sephadex G-100 (Sigma). Hemoglobin species [23] or [24] at about 1 mM in heme units was deoxygenated by gentle shaking of the sample under a flow of O_2-free nitrogen for 1.5 h at 4 °C. The sample was then transferred into a Coy Laboratory Products Type B anaerobic chamber and gentle shaking was carried out for another 15 min at a temperature slightly below 10 °C to ensure complete deoxygenation. The sample was diluted into standard buffer which had been exhaustively deoxygenated within the anaerobic chamber for at least 48 h and equilibrated for 30 min at the temperature of each experiment. Before the sample was loaded onto a column, an aliquot of the diluted hemoglobin was analyzed spectrophotometrically for total Hb concentration and extent of deoxygenation. The procedure for preparing samples of species [41] was similar to that for species [23] and [24] except that [41] was not subjected to the deoxygenation procedure since this species does not bind O_2. The column and the samples were maintained within ±0.05 °C of the temperature of each experiment by a Lauda K-2/R thermoregulator (Brinkmann Instruments). Oxygen partial pressure inside the chamber was monitored with a Coy Model 10 gas analyzer and never exceeded the 1 ppm detection limit. Elution profiles of the hemoglobins were monitored inside the chamber with a Shimadzu UV-150-02 spectrophotometer. The elution volume V_e at each plateau Hb concentration was determined for the equivalent sharp boundaries on leading and trailing edges of the "large-zone" elution profile. The equivalent sharp boundaries were measured as centroids by numerical integration (Valdes & Ackers, 1977). These elution volumes were transformed into weight-average partition coefficients $\bar{\sigma}_w$:

$$\bar{\sigma}_w = \frac{V_e - V_0}{V_i} \quad (7)$$

where V_0 and V_i are the void and internal volumes, respectively. They were measured from "small-zone" experiments using blue dextran (Sigma) and glycylglycine (Mann Research Laboratories), respectively. For Hb dimer−tetramer equilibrium, $\bar{\sigma}_w$ at a given Hb concentration depends on the fractions of dimer (f_D) and tetramer (f_T) and their

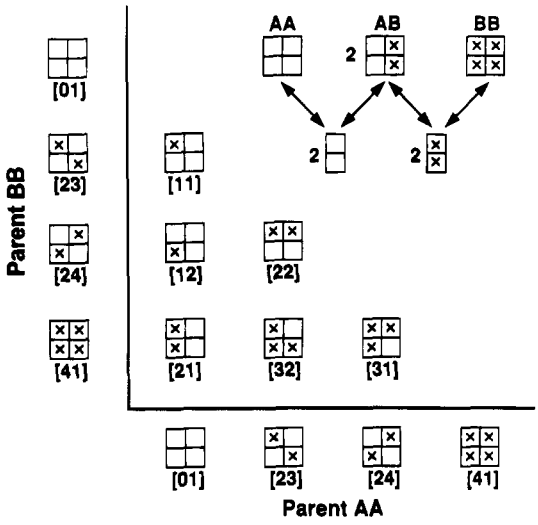

FIGURE 3: Hybridization scheme for construction of the six hybrid species from their parent molecules.

individual species partition coefficients σ_D and σ_T:

$$\bar{\sigma}_w = \sigma_D f_D + \sigma_T f_T \tag{8}$$

Here, the fraction f_D is

$$f_D = \frac{-1 + (1 + 4K_2P_t)^{1/2}}{2K_2P_t} \tag{9}$$

where P_t is total heme concentration and K_2 is the equilibrium constant for dimer−tetramer assembly. The $\bar{\sigma}_w$ data were analyzed according to eq 8 by the nonlinear least-squares program NONLIN (Johnson & Frasier, 1985).

Preparation of Hybrid Hemoglobins. Six of the 10 ligation microstates of hemoglobin, species [11], [12], [21], [22], [31], and [32], were studied in hybrid mixtures (see Figure 3 for construction of these hybrid species). For example, species [21] $(\alpha^{+CN}\beta^{+CN})(\alpha\beta)$ was prepared by mixing parent species [01] $(\alpha\beta)_2$ and [41] $(\alpha^{+CN}\beta^{+CN})_2$. The two parent species undergo a dimer rearrangement reaction that yields species [21] as a hybrid tetramer in the presence of the two original parent species. To form a hybrid, the two parent species were first deoxygenated by gentle shaking of the samples under a flow of O_2-free nitrogen for 1.5 h at 4 °C. The samples were immediately transferred into a N_2 glove bag. Deoxygenated glucose oxidase (Sigma), *Aspergillus niger* catalase (Sigma), and glucose (Sigma) were added into the two deoxygenated parent hemoglobin samples and the samples were allowed to stand at room temperature for 10 min inside the N_2 glove bag to ensure complete removal of O_2. The final concentrations of glucose oxidase, catalase, and glucose were 1.8 mg/mL, 0.3 mg/mL, and 0.6%, respectively. The two parent hemoglobins were mixed and then aliquotted into septum-sealed vials. The vials were immersed in 0.1% sodium dithionite solution within a crimp-sealed serum vial. The samples in the double-sealed vials were incubated at a given temperature. The approach to and maintenance of equilibrium of the hybrid mixture were verified by assaying the distribution of tetrameric species as a function of time with cryogenic isoelectric focusing (LiCata et al., 1990). To facilitate electrophoretic resolution, one of the parent species in each hybrid mixture was prepared using HbS (β6 Glu → Val) in which the mutation site is located away from the dimer−dimer interface. Additional controls indicated no effect of the β^s subunits on resolved energetics (LiCata et al., 1990). The total hemoglobin concentration during incubation of the hybrid mixture was approximately 1 mM in heme units.

Calculation of Assembly Enthalpies and Entropies for Hybrid Species. For each of the six hybrid species, the hybridization equilibrium free energy at a given temperature was analyzed in terms of the deviation free energy δ, which measures the difference between the actual hybrid (AB) assembly free energy ($^{AB}\Delta G_2$) and the mean of the assembly free energies of the two parent species (AA and BB):

$$\delta = {}^{AB}\Delta G_2 - {}^1/_2({}^{AA}\Delta G_2 + {}^{BB}\Delta G_2) \tag{10}$$

The deviation free energy δ at a given temperature can be calculated directly from equilibrium fractions of a hybrid (f_{AB}) and its two parent species (f_{AA} and f_{BB}) (LiCata et al., 1990):

$$\delta = -RT \ln \frac{f_{AB}}{2(f_{AA}f_{BB})^{1/2}} \tag{11}$$

These fractions were measured from optical scanning of cryogenic isoelectric focusing gels and reflected the species equilibrium distributions in an incubation mixture at a given temperature T. Assembly free energy of the hybrid species is, by definition

$$^{AB}\Delta G_2 = {}^{AB}G_{tet} - {}^{A}G_{dimer} - {}^{B}G_{dimer} \tag{12}$$

where terms on the right denote free energies of all species in the assembly reaction. Substituting eq 12 (and the corresponding equations for $^{AA}\Delta G_2$ and $^{BB}\Delta G_2$) into eq 10, we obtain (Doyle & Ackers, 1992)

$$\delta = {}^{AB}G_{tet} - {}^1/_2({}^{AA}G_{tet} + {}^{BB}G_{tet}) \tag{13}$$

The partial derivative of δ/T with respect to temperature T at constant pressure gives

$$\left[\frac{\partial \frac{\delta}{T}}{\partial T}\right]_P = \left[\frac{\partial \frac{{}^{AB}G_{tet}}{T}}{\partial T}\right]_P - \frac{1}{2}\left\{\left[\frac{\partial \frac{{}^{AA}G_{tet}}{T}}{\partial T}\right]_P + \left[\frac{\partial \frac{{}^{BB}G_{tet}}{T}}{\partial T}\right]_P\right\} \tag{14}$$

Applying the Gibbs−Helmholtz relation to eq 14 gives

$$\left[\frac{\partial \frac{\delta}{T}}{\partial T}\right]_P = -\frac{{}^{AB}H_{tet}}{T^2} + \frac{1}{2}\left(\frac{{}^{AA}H_{tet}}{T^2} + \frac{{}^{BB}H_{tet}}{T^2}\right) \tag{15}$$

By multiplying eq 15 by $-T^2$ and introducing dimer enthalpies $^{A}H_{dimer}$ and $^{B}H_{dimer}$, we see that

$$-T^2\left[\frac{\partial \frac{\delta}{T}}{\partial T}\right]_P = {}^{AB}\Delta H_2 - {}^1/_2({}^{AA}\Delta H_2 + {}^{BB}\Delta H_2) \tag{16}$$

where ΔH terms denote assembly enthalpies of the three respective tetramer species (i.e., $^{AB}\Delta H_2 = {}^{AB}H_{tet} - {}^{A}H_{dimer} - {}^{B}H_{dimer}$, etc.).

Similarly, by taking the partial derivative of the "deviation energy" δ with respect to T at constant pressure, we have an entropic relationship among the three tetrameric species in hybrid equilibrium:

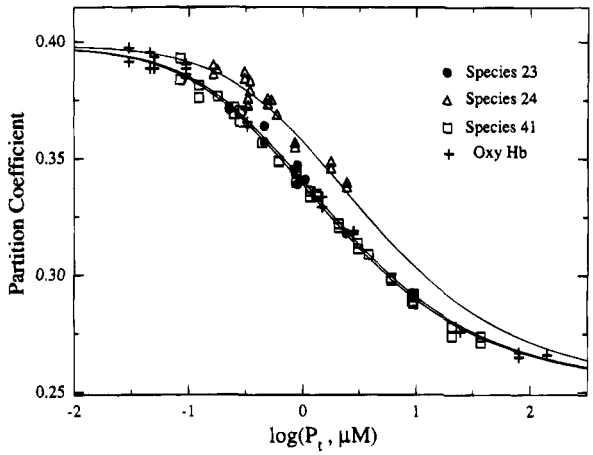

FIGURE 4: Analytical gel chromatography results showing weight-average partition coefficients versus Hb concentrations in units of micromolar heme. Data for species [23] (●), [24] (△), and [41] (□) were obtained anaerobically at 26 °C. Curves represent best-fit parameters from global analysis for the respective dimer−tetramer equilibria of each species. The asymptotic dimer and tetramer partition coefficients were 0.398 and 0.253, respectively. Data for oxyHb (+) measured at 21.5 °C are included for comparison. The two data points at each Hb concentration correspond to the leading and trailing edges of each elution profile. Solution conditions are 0.1 M Tris-HCl, 0.1 M NaCl, 1 mM Na_2-EDTA, and 10 μM KCN, pH 7.40.

$$\left(\frac{\partial\delta}{\partial T}\right)_p = -{}^{AB}\Delta S_2 + {}^1/_2({}^{AA}\Delta S_2 + {}^{BB}\Delta S_2) \qquad (17)$$

Equations 16 and 17, which represent alternative forms of the Gibbs−Helmholtz equation, provide a thermodynamic basis for evaluating the assembly enthalpies and entropies of each hybrid species.

RESULTS

Temperature Dependence of Assembly Free Energies. For species [23], [24], and [41], the determination of equilibrium constants K_2 by eqs 7−9 required the respective partition coefficients representing pure dimeric and tetrameric species. To achieve high resolution of these end-state parameters, at least 12 zones were obtained at each temperature, employing 3 orders of magnitude range in concentration of species [41]. These data, in combination with similar data on species [23] and [24] at three or more Hb concentrations, were analyzed globally to obtain common dimer and tetramer partition coefficients for all three ligation species. Confidence intervals obtained at each temperature thus included the uncertainty from "floating" σ_D and σ_T during analysis. However, to avoid potential effects of changing temperature on σ_D and σ_T, global regression analysis was only performed on combined data at the same temperature. Thus σ_D and σ_T were not constrained to common values over the experimental range (5−26 °C). Figure 4 shows the data at 26 °C along with curves representing the global-analysis best-fit parameters for assembly equilibria of the three ligation species. To ensure valid determination of dimer and tetramer partition coefficients and of K_2 for species [23], [24], or [41], we carried out similar experiments at 21.5 °C on the same column using oxygenated hemoglobin A_0 (oxyHb). Those results are also given for comparison in Figure 4. The resolved assembly free energy of oxyHb was −8.10 ± 0.10 kcal/mol at 21.5 °C, in agreement with the previously determined −8.05 ± 0.10 kcal/mol (Chu et al., 1984). Void and internal volumes of each column measured before and after the Hb experiments at each temperature indicated no significant changes.

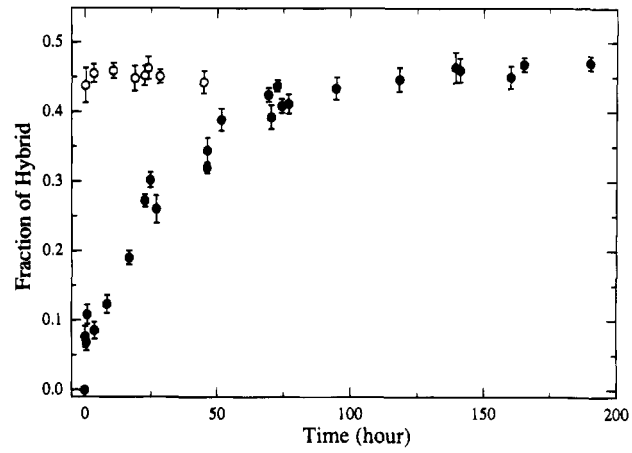

FIGURE 5: Time course for formation of hybrid species [21] (●) and [22] (○). For each hybrid species the initial ratio of parent species was approximately 1:1.

Prolonged exposure of dilute species [24] samples (i.e. <10 μM) to higher temperatures (>21.5 °C) during anaerobic deoxygenation and sample loading gave inconsistent boundary positions. Apparently greater association was estimated from trailing boundaries than from leading boundaries. Spectra of these samples in the visible region showed unexpected changes upon prolonged exposure to high temperature, suggesting degradation. The long-term effect of temperature on dilute solutions of species [23] and [41] was much less pronounced but became significant at 26 °C. To minimize degradation during runs at 21.5 and 26 °C, all samples were kept below 10 °C during deoxygenation and during sample loading within the anaerobic chamber. Loading was carried out by pipetting only 1−2 mL of the sample each time and loading it on the column after warming it up for 1−3 min at room temperature. This procedure resulted in consistent positions for the loading and trailing boundaries within the error shown in Figure 4. We believe that this "more gentle" procedure leads to a significantly more accurate estimate of the assembly equilibrium constant. The resulting free energy for species [24] at 21.5 °C is found to be 0.5 kcal less negative than determined previously (Smith & Ackers, 1985). On the other hand, the ΔG_2 values determined at the same temperature for species [23] (−8.38 ± 0.10 kcal/mol) and species [41] (−8.34 ± 0.10 kcal/mol) agree closely with those previously determined, i.e., −8.2 ± 0.2 and −8.5 ± 0.2 kcal/mol, respectively (Smith & Ackers, 1985). Figure 4 shows that dimer−tetramer assembly of species [24] is energetically less favorable than that of species [23] or [41].

Each of the six ligation species with dissimilar dimeric halves (i.e., [11], [12], [21], [22], [31], and [32]) must be studied in hybrid equilibrium with its appropriate pair of parental species. The fractions of each hybrid and of its parents were determined by cryogenic isoelectric focusing (LiCata et al., 1990). The ${}^{AB}\Delta G_2$ values for each hybrid were calculated by eqs 10 and 11. Approach to equilibrium in formation of hybrid species [22], [31], or [32] was rapid (i.e., within an hour) at all temperatures studied. Equilibration times for species [11], [12], or [21] ranged from 10 h at 26 °C to several weeks at low temperature. As much as 5 weeks was required for species [21] to achieve its equilibrium distribution at 5 °C. Figure 5 shows the hybridization time

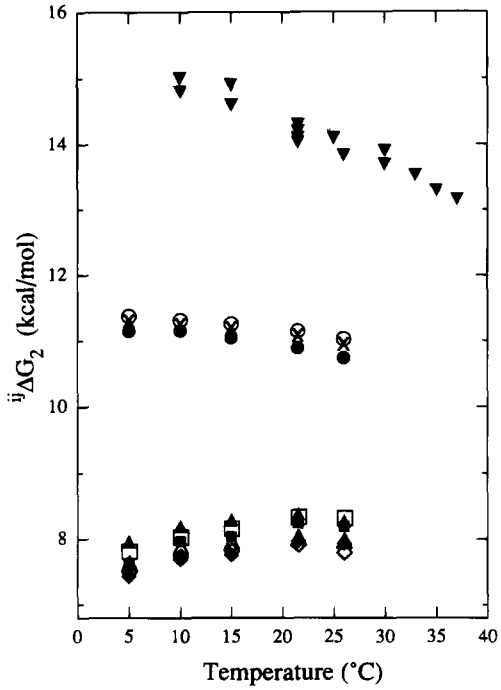

FIGURE 6: Assembly free energies of the 10 cyanomet ligation species versus temperature. Data for species [11] (×), [12] (●), [21] (○), [22] (△), [31] (◆), and [32] (■) were determined by cryogenic isoelectric focusing of hybrid mixture experiments. Data for species [23] (▲), [24] (◇), and [41] (□) were obtained using analytical gel chromatography. Data for species [01] (▼) are the previous work of Ip and Ackers (1977), Turner (1989), and Johnson (1990). Solution conditions are 0.1 M Tris-HCl, 0.1 M NaCl (0.18 M total chloride), 1 mM Na_2EDTA, and 10 μM KCN, pH 7.40.

courses for species [21] and [22] at 21.5 °C. Formation of species [22] reaches equilibrium within a few minutes, whereas about 100 h is required for species [21]. This finding is especially interesting since species [21] and [22] are identical in terms of chemical composition, while differing only in the configuration of ligated subunits (Figure 1). To prevent O_2 diffusion into samples in those extremely long incubation experiments at low temperature, up to 0.5% sodium dithionite was used as an oxygen scavenger in the double-sealed vials. Sample integrity after long-time incubation was verified in the isoelectric focusing gel and by spectrophotometry of the sample in the visible region. It was found that deviation free energies of all six hybrid species were in the range of 0.0−0.2 kcal between temperatures of 5 and 26 °C (data not shown). These results indicate almost exact energetic additivity of the hybrid species for all temperatures studied at pH 7.4, i.e., the free energy of assembly for the hybrid species equals the mean of the assembly free energies of the parent species to within experimental error.

Standard Gibbs energies, $^{ij}\Delta G_2$, of dimer−tetramer assembly for the 10 ligation microstates of hemoglobin at various temperatures are given in Figure 6. Shown for species [01] are the previously determined values of Ip and Ackers (1977), Turner (1989), and Johnson (1990). At each temperature the 10 species are found to exhibit three discrete free energy levels with a specific combinatorial distribution (i.e., with species [01] solely at the top, the six species [22], [23], [24], [31], [32], and [41] at the bottom level; a third (intermediate) level is occupied by species [11], [12], and [21]). Of particular interest is the finding that the four doubly ligated species are always split into two free energy levels

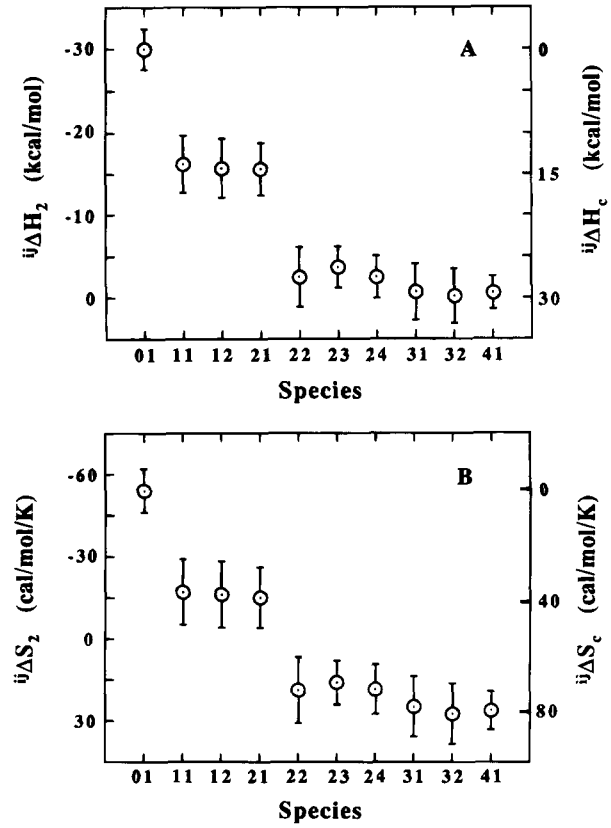

FIGURE 7: (A) Distributions of assembly enthalpy (left ordinate) and cooperative enthalpy (right ordinate) of the 10 cyanomet ligation species of Hb. (B) Distributions of assembly entropy (left ordinate) and cooperative entropy (right ordinate) of the 10 cyanomet ligation species of Hb at 21.5 °C.

with species [21] different from the other three species. This distribution pattern is found at every temperature studied, while the energetic distance between the levels increases with decreasing temperature. It is seen (Figure 6) that assembly free energies of all 10 species show nearly linear dependencies on temperature within the range studied.

Enthalpic and Entropic Components of the Assembly Free Energies. Temperature dependence of the equilibrium constants for assembly of "symmetric" species [23], [24], and [41] were analyzed using the van't Hoff equation (eq 18) to yield assembly enthalpies, $^{ij}\Delta H_2$:

$$\frac{\partial \ln {}^{ij}K_2}{\partial T} = \frac{{}^{ij}\Delta H_2}{RT^2} \tag{18}$$

From the determined values of $^{ij}\Delta H_2$ and $^{ij}\Delta G_2$, corresponding entropies $^{ij}\Delta S_2$ for assembly of species [23], [24], and [41] were calculated ($^{ij}\Delta G_2 = {}^{ij}\Delta H_2 - T^{ij}\Delta S_2$). These are shown in Figure 7 along with enthalpies and entropies for assembly of the six hybrid species that were analyzed using eqs 16 and 17. The term on the left of eq 16 denotes temperature dependence of deviation free energies. These also exhibited linear van't Hoff relationships within the range studied for all six hybrid species (data not shown). Enthalpies and entropies of the parent species on the right side of eqs 16 and 17 were determined independently, as described above. Figure 7 shows clearly that the enthalpies of assembly and also the entropies of assembly distribute into three discrete levels for the 10 ligation species. These distributions follow an identical pattern to hose of assembly free energies (or of cooperative free energies). Species [21]

Table 3: Thermodynamic Parameters for Quaternary Assembly[a] of Human Hemoglobin Ligation Species

species[b]	$^{ij}\Delta G_2$ (kcal/mol)	$^{ij}\Delta H_2$ (kcal/mol)	$-T^{ij}\Delta S_2$ (kcal/mol)	$^{ij}\Delta S_2$ (cal mol^{-1} deg^{-1})
[01]	-14.3 ± 0.2	-30 ± 2	16 ± 2	-54 ± 8
[11]	-11.3 ± 0.2	-16 ± 3	5 ± 3	-17 ± 12
[12]	-11.0 ± 0.2	-16 ± 3	5 ± 3	-16 ± 12
[21]	-11.2 ± 0.2	-16 ± 3	5 ± 3	-16 ± 11
[22]	-8.0 ± 0.2	-2 ± 3	-6 ± 3	19 ± 12
[23]	-8.4 ± 0.2	-3 ± 2	-5 ± 2	16 ± 8
[24]	-7.9 ± 0.2	-3 ± 2	-5 ± 2	18 ± 9
[31]	-8.0 ± 0.2	-1 ± 3	-7 ± 3	25 ± 11
[32]	-8.2 ± 0.2	0 ± 3	-8 ± 3	27 ± 11
[41]	-8.3 ± 0.2	-1 ± 2	-8 ± 2	26 ± 7

[a] Derived from standard-state equilibrium constants for assembly of each tetrameric species [*ij*] from its constituent $\alpha\beta$ dimeric half-molecules to form the "$\alpha^1\beta^2$ interface". [b] Species depicted topographically in Figure 1 where ligated sites (denoted by X) have cyanomethemes.

has very different enthalpy and entropy values from the other doubly ligated species, while the two singly ligated species and species [21] occupy a common level with respect to both enthalpy and entropy. The assembly enthalpies and entropies of species [01], [11], [12], and [21] are large and negative. By contrast, assembly of the other species revealed large positive entropy and a near zero enthalpy. Numerical values of these thermodynamic parameters are given in Table 3.

Cooperative Enthalpies and Entropies for Stepwise Cyanomet Ligation. Values of the $^{ij}\Delta H_c$ and $^{ij}\Delta S_c$ for each of the nine ligated species are given in Figure 7. The total ranges of these parameters (over ligation of all four sites) is readily determined as $^{41}\Delta H_c$ and $^{41}\Delta S_c$ using eqs 5 and 6. These values for full cyanomet ligation of tetrameric hemoglobin were found to be 29 ± 4 kcal/mol and 80 ± 15 cal mol^{-1} K^{-1}, respectively.

To see how this "total cooperative enthalpy" and "total cooperative entropy" are spent on stepwise increments along the various ligation pathways, each stepwise value of cooperative enthalpy and of cooperative entropy was evaluated as the difference in $^{ij}\Delta H_2$ (or $^{ij}\Delta S_2$) in a given pathway relative to the preceding ligation species along the same pathway. The 16 stepwise values are designated ΔH_c^s or ΔS_c^s, where s denotes the reaction step number in Figure 1. Figure 8 shows these values along with stepwise cooperative free energies for two illustrative ligation pathways. Under these conditions (pH 7.4) approximately half of the total cooperative enthalpy and cooperative entropy are spent on the first ligation step (binding either to an α or to a β subunit). The other half is spent at a ligation step which creates a molecule with ligated subunits on both dimeric half-molecules. It is seen that the cooperative free energies manifested in the first and third ligation steps of pathway A and the first and second ligation steps of pathway B are composed of large unfavorable enthalpic changes and large favorable entropic changes. Table 2 shows the mean values of the enthalpic and entropic components for each synchronized cluster of transitions according to eq 4. It is seen that (a) the tc and sw values are tightly clustered around large values, as is the overall transition (T $\rightarrow$ R), (b) the eight null transitions have values tightly clustered around zero, both for the enthalpic and entropic contribution, (c) the net free energy of tertiary constraint is enthalpic, and the same is true of the switch point free energy, and finally (d) the 6 kcal of overall cooperative free energy is a result of enthalpic dominance.

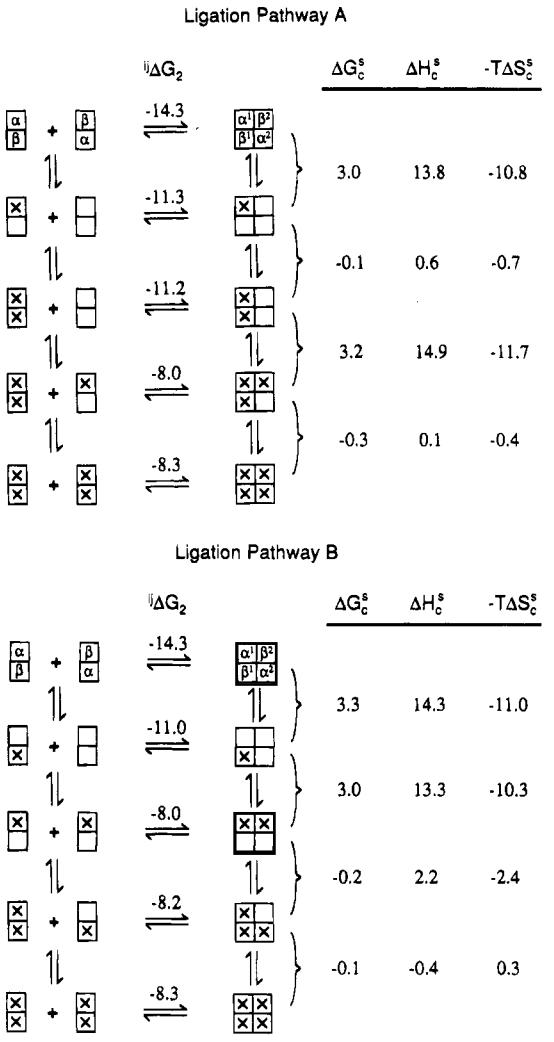

FIGURE 8: Enthalpic and entropic components of the stepwise cooperative free energies for two representative ligation pathways at 21.5 °C (subunit arrangement in tetrameric Hb as in Figure 1). Free energies ($^{ij}\Delta G_2$) are also shown for the respective dimer–tetramer assembly reactions.

Accuracy of Thermodynamic Parameters. The enthalpies and entropies for assembly of species [41] were found in this study to differ significantly from a preliminary estimate (Daugherty et al., 1991) which was based on data over a limited temperature range of 21.5–35 °C. The effects of high temperature on sample integrity discussed above and the relatively narrow range of temperature employed are believed to be major factors contributing to an incorrect estimation of ΔH_2 and ΔS_2 that was obtained for species [41]. The enthalpy and entropy for assembly of species [01] under these conditions has been determined previously (Ip & Ackers, 1977; Turner, 1989; Johnson, 1990), with results that are highly consistent with the present study (Figure 6).

For the six hybrid species, we found that using van't Hoff analysis on their assembly free energies to estimate $^{ij}\Delta H_2$ and $^{ij}\Delta S_2$ resulted in underestimate of the errors. Such analysis does not properly include the propagation of errors in assembly enthalpies and entropies of the parent species which are of necessity part of the reaction system. Use of the Gibbs–Helmholtz eqs 16 and 17 provides more realistic error estimates. The enthalpy and entropy evaluated for species [21] were found to be significantly less negative than previously estimated from data over a limited temperature range of 21.5–35 °C. The effects of high temperature on

Table 4: Stagewise Distributions of Thermodynamic Parameters for Human Hemoglobin

(A) Enthalpies and Entropies of Dimer−Tetramer Assembly[a]

	cyanomet system		oxygen system[b]	
ligands bound	$^{i}\Delta H_2$	$^{i}\Delta S_2$	$^{i}\Delta H_2$	$^{i}\Delta S_2$
0	−30 ± 2.5	−54 ± 8	−30 ± 2.5	−54 ± 8
1	−16 ± 4	−18 ± 12	−18 ± 1	−21 ± 3
2	−15 ± 4	−17 ± 12	−15 ± 8	−23 ± 10
3	0 ± 3	26 ± 11	3 ± 4	35 ± 12
4	−1 ± 2	26 ± 6	4 ± 2	40 ± 6

(B) Cooperative Enthalpies and Entropies for Heme Site Ligation

	cyanomet system		oxygen system	
ligands bound	$^{i}\Delta H_c$	$^{i}\Delta S_c$	$^{i}\Delta H_c$	$^{i}\Delta S_c$
0	0	0	0	0
1	14 ± 4	36 ± 14	12 ± 3	33 ± 9
2	15 ± 4	37 ± 14	15 ± 8	31 ± 13
3	30 ± 4	80 ± 14	33 ± 5	89 ± 14
4	29 ± 3	80 ± 10	34 ± 3	94 ± 10

[a] Conditions: pH 7.4, 21.5 °C, 0.1 M Tris-HCl, 0.1 M NaCl, and 1 mM EDTA. [b] Data from Mills and Ackers (1979).

sample integrity and narrow experimental range are believed to be sources of error in those preliminary estimates. The haptoglobin kinetic technique (Ip & Ackers, 1977) for tetramer−dimer dissociation rates of species [01] has been used for the unligated species [01] in both the preliminary studies and in the present work. This technique has been found valid over a wide range of Hb systems and conditions [cf. Turner et al. (1992)].

Comparison with Stagewise Oxygen Ligation Distributions. To compare temperature dependence of cooperative free energies manifested in the Fe(II)/Fe(III)-CN system with corresponding effects in the Fe(II)/F(II)-O_2 system,[4] we calculated the average free energy of assembly (and cooperativity) for each stage of cyanomet ligation. For example, values of the average assembly equilibrium constant for the four doubly ligated species ($\overline{^{2}K_2}$) were determined by the relationship (Ackers et al., 1992)

$$\overline{^{2}K_2} = {}^{1}/_{6}(2^{21}K_2 + 2^{22}K_2 + {}^{23}K_2 + {}^{24}K_2) \qquad (19)$$

where $^{2j}K_2$ ($j = 1-4$) is the assembly equilibrium constant for species $2j$. van' Hoff analysis of the $\overline{^{i}K_2}$ data results in the average assembly enthalpy $\overline{^{i}\Delta H_2}$ and entropy $\overline{^{i}\Delta S_2}$ for ligation stage i. These are shown in Table 4 along with the stagewise assembly enthalpies and entropies for partially oxygenated hemoglobin (Mills & Ackers, 1979). It is currently impossible to explicitly resolve cooperative free energies, enthalpies, and entropies for each ligation microstate in the oxygenation system due to rapid exchange of site-bound O_2 molecules and the tetramer−dimer dissociation/disproportionation. From the detailed values in Table 3, the cooperative enthalpies ($^{i}\Delta H_c$) and entropies ($^{i}\Delta S_c$) for each ligation stage were calculated using relationships similar to eqs 5 and 6, and the resulting values are given in Table 4. Despite the numerical uncertainty shown, values in Table 4 clearly indicate a common pattern of temperature effects on dimer−tetramer assembly as well as cooperativity in the two ligation systems.

DISCUSSION

To evaluate cooperativity of heme site ligation even though binding affinity is too strong for direct measurements, we utilized the approach, outlined in the introduction, which takes advantage of thermodynamic linkage between ligation reactions and subunit assembly: the energetic costs of cooperativity are measured by the respective energy differences for assembly of a ligation species ij relative to unligated species [01]. The findings presented here clearly show that (a) the previously observed combinatorial nature of cooperative free energies for the 10 ligation species is also manifested individually by the cooperative enthalpies and cooperative entropies, (b) their distributions obtained with cyanomet ligation are highly consistent with previous determinations of the stagewise parameters with oxygen binding, and (c) the dramatic phasing and synchronization of responses found previously with cooperative free energies and Bohr protons for specific configurational transitions of ligated sites are also manifested by the cooperative enthalpies and cooperative entropies. Additional probing of symmetry rule behavior may be explored through certain correlations among these parameters.

Correlation of Cooperative Enthalpies with Bohr Proton Release. Previous experimental work on thermodynamics of the oxygen-linked Bohr effect has revealed two notable features: (a) The apparent heat of Bohr proton release was unexpectedly large, i.e. 11−15 kcal/mol of H^+ at pH 7.4 (Antonini et al., 1965; Chipperfield et al., 1967; Rollema et al., 1975; Chu et al., 1984). This magnitude exceeds the standard ionization heats for amino acid side chains that are expected to contribute (i.e., with pK_a values in the range 6.5−8, such as histidines or N-terminal amino groups). This finding suggests that the apparent enthalpy may also reflect other processes that are driven in parallel with Bohr proton release. (b) The apparent ΔH of Bohr proton release at pH 7.4 was found to be approximately proportional to the number of protons released (Mills et al., 1979; Mills & Ackers, 1979; Ackers, 1980; Chu et al., 1984), also suggesting that the linkages between heme site ligation and Bohr protons have a global character.

For the cyanomet species of this study, we analyzed the correlation of cooperative enthalpies with Bohr proton linkages through the cascade of all 16 ligation steps which connect the 10 species. Stepwse cooperative enthalpies (ΔH_c^s) were evaluated from assembly enthalpies for each of the appropriate microstates ($\Delta H_c^s = {}^{ij}\Delta H_2 - {}^{(i-l)k}\Delta H_2$) similarly to that of the cooperative free energies. Stepwise Bohr proton release in tetramers relative to dimers ($\Delta \nu_c^s$) was evaluated from the proton release values ($^{ij}\Delta \nu_2$) which accompany dimer−tetramer assembly (Daugherty et al., 1994) ($\Delta \nu_c^s = {}^{ij}\Delta \nu_2 - {}^{(i-l)k}\Delta \nu_2$). In view of previous observations with stagewise oxygenation (Chu et al., 1984), it was of interest to examine whether the stepwise cooperative enthalpies were linearly correlated with the corresponding numbers of Bohr protons, as prescribed by

$$\Delta H_c^s = \Delta H_c' + (\Delta H_{H^+})(\Delta \nu_c^s) \qquad (20)$$

where $\Delta H_c'$ denotes cooperative enthalpy in the absence of Bohr proton release; the slope (ΔH_{H^+}) denotes apparent heat for Bohr protons released per mole of ligand bound in tetramers relative to dimers. It must be noted that this "difference enthalpy" of ligand-induced proton release includes not just the local side chain deprotonation heats from amino acid "Bohr groups" but also the heats of any other ionic, solvation, or structural effects that may be synchronized with Bohr proton release.

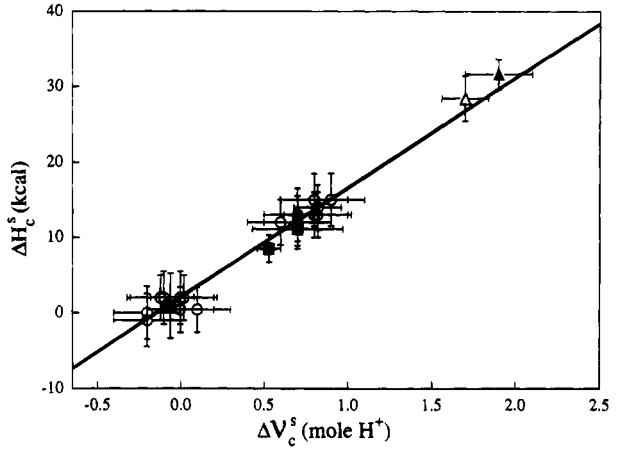

FIGURE 9: Correlation of stepwise cooperative enthalpies, ΔH_c^s, with stepwise Bohr proton release, $\Delta \nu_c^s$, in tetramers relative to dimers at 21.5 °C and pH 7.4. Open circles denote stepwise cyanomet ligation. Open triangles correspond to full cyanomet ligation (all four heme sites). Filled squares denote stagewise oxygenation (i.e., all microstates with the same number of oxygen bound). Filled triangles are for full oxygenation (binding four oxygens). Horizontal and vertical error bars represent standard deviations in $\Delta \nu_c^s$ and ΔH_c^s, respectively. Solid line is the linear least-squares fit for stepwise ligation in the cyanomet system (open circles).

Figure 9 shows a plot of ΔH_c^s versus $\Delta \nu_c^s$ for the 16 stepwise transitions (Figure 1). Vertical and horizontal error bars denote standard deviations in the ΔH_c^s and $\Delta \nu_c^s$ values, respectively. For ΔH_c^s the error is ±3.5 kcal/mol of bound ligand, and for $\Delta \nu_c^s$ it is ±0.2 mol of H^+/mol of bound ligand. Least-squares analysis by eq 20 yielded the solid line representing the best fit slope of 14.5 ± 1.4 kcal/mol and intercept at 2.0 ± 0.8 kcal/mol. By eq 20, these values respectively represent the heat of Bohr proton release ΔH_{H^+} per binding step and the non-proton-linked part of the cooperative enthalpy.

A conspicuous feature is that the stepwise heats ΔH_c^s are clustered around two values of proton release. One cluster is at $\Delta \nu_c^s = 0.0 \pm 0.2$, while the other is at $\Delta \nu_c^s = 0.7 \pm 0.2$. In addition, the "overall" cooperative enthalpy (i.e., for ligation of all four sites in tetramers minus that of their dissociated dimers is plotted against Bohr proton release. This value is seen to occupy a nearly collinear position on the same plot with the stepwise increments (Figure 9). Thus for each ligation step, or combination thereof, the reduction of cooperative enthalpy is equivalent to the apparent heat of Bohr proton release as found previously for stagewise binding of oxygen under the same conditions (Chu et al., 1984).

To compare cyanomet ligation with oxygen ligation more closely, we calculated the stagewise cooperative enthalpies from the previously reported experimental enthalpies of binding oxygen by tetramers and dimers (Mills & Ackers, 1979; Chu et al., 1984) and the reported Bohr protons for oxygen binding to tetramers relative to dimers (Chu et al., 1984). These results are given as solid points in Figure 9 along with overall cooperative enthalpy versus Bohr proton release. It is seen that both ligation systems exhibit the same correlation between ΔH_c and $\Delta \nu_c$, within experimental error, and that the reduction of binding enthalpy in tetramers relative to dimers can be accounted for by the same heat effect in both ligation systems (14.5 ± 1.4 kcal mol^{-1} (mol of $H^+)^{-1}$]. This result strongly supports the premise that the enthalpy/proton linkage is a fundamental property of the protein but not the type of heme site ligand.

Correspondence with Symmetry Rule Mechanism. The values plotted in Figure 9 for the 16 stepwise transitions fall into distinct clusters which correspond with predictions of the symmetry rule mechanism:

(a) Clustered near the origin of this plot are the ligand-induced heat and proton effects of the eight stepwise transitions within R and within T which, by the symmetry rule mechanism, are predicted not to generate quaternary switching (i.e., reactions 9, 12, 13, 14, 15, and 16 of Figure 1) nor tertiary constraint (i.e., reactions 4 and 6). These ligation steps are predicted to have no Bohr proton release in excess of the dimeric values, and this has been found to be the case (Daugherty et al., 1994).

(b) The remaining eight stepwise values are clustered around a central value of the plot (where $\Delta H_c^s = 14 \pm 3$ kcal; $\Delta \nu_c^s = 0.7 \pm 0.2$ mol of H^+/mol of ligand bound). According to the symmetry rule mechanism, these transitions reflect two kinds of molecular processes: (i) the two transitions which generate tertiary constraint (reactions 1 and 2) and (ii) the six switch point transitions (reactions 3, 5, 7, 8, 10, and 11) where the (energetically favorable) release of tertiary constraint as the T interface is broken is energetically opposed by the unfavorable T → R rearrangement of the interface itself. The ΔH_c^s and $\Delta \nu_c^s$ values reflect these switch point transition responses, which are linked by eq 4:

$$\Delta H_c^{sw} = \Delta H_c^{T \rightarrow R} - \Delta H_c^{tc} \quad (21)$$

$$\Delta \nu_c^{sw} = \Delta \nu_c^{T \rightarrow R} - \Delta \nu_c^{tc} \quad (22)$$

At the upper right-hand corner of Figure 9, the overall cyanomet ligation point lies at approximately twice the distance from the origin (along the solid line) as the cluster of eight transitions which alter molecular constraints (i.e., the tc and sw transitions). Additivity of these quantities is, of course, a necessary result for each pathway of complete ligation (i.e., from species 01 → 41). However, the symmetry rule mechanism predicts that essentially the same final value will be achieved whenever a ligation pathway (from 01) leads to ligation of both dimeric half-molecules; it also specifically predicts the eight null transitions where no cooperativity responses will occur. It is clear from the results of this study, as shown in Figure 9 (also Tables 1 and 2), that both of these predictions are fulfilled. Under these pH conditions the enthalpic terms for tertiary constraint ΔH_{tc} and for the switch point transitions ΔH_{sw} have approximately equal magnitude. Thus when a net 15 kcal/mol is spent at each switch point transition but the molecule also has relinquished 15 kcal/mol of previously stored ΔH_{tc}, the value of $\Delta H_{T \rightarrow R}$ is 30 kcal/mol.

By contrast, a plot of stepwise cooperative enthalpies versus stepwise Bohr free energies (Figure 10) shows clear-cut separation of the eight transitions in group (b) since the tertiary and quaternary Bohr effects have distinctly unequal free energies at pH 7.4 (Daugherty et al., 1994). The transitions which generate tertiary constraint (i.e., reactions 1 and 2) are each accompanied by 0.7 ± 0.3 kcal (the "tertiary Bohr free energy"), while the overall Bohr free energy at pH 7.4 is 3.0 ± 0.2 kcal. By contrast, each of the six switch point transitions is found to generate 2.3 kcal of proton-linked free energy, ΔG_{Bohr}^{sw}. However, both pro-

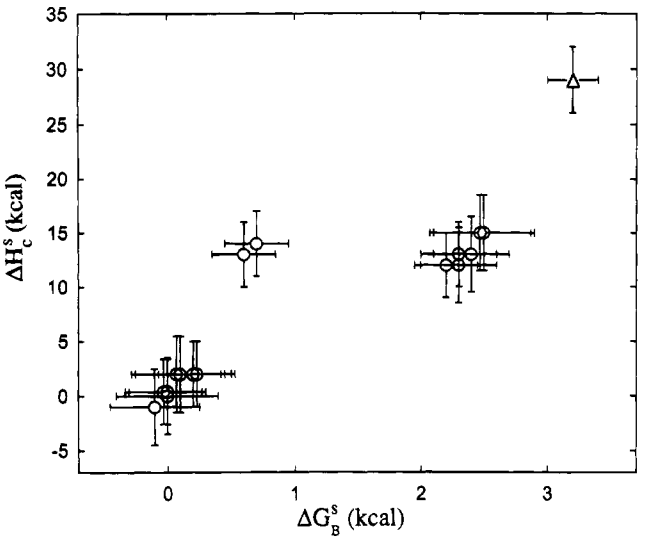

FIGURE 10: Correlation of stepwise cooperative enthalpies ΔH_c^s (obtained in this study) with stepwise Bohr free energies [from Daugherty et al. (1994)]. Circles represent stepwise ligation. Triangles represent overall ligation.

cesses happen to yield the same enthalpic change (~14 kcal). The upper right-hand point on Figure 10 which represents overall ligation (i.e., all four heme sites) thus reflects the net result of the interplay between the tertiary constraint and switchpoint contributions. The enthalpic coordinate of this point is the sum of enthalpies for the two processes. On the Bohr free energy coordinate, its value is a sum over the two processes, i.e., 3.0 = 0.7 + 2.3 (in kilocalories). This is an expected result from the symmetry rule mechanism since the Bohr energy of quaternary T → R switching is also given by eq 4, $\Delta G_{Bohr}^{T\rightarrow R} = \Delta G_{Bohr}^{tc} + \Delta G_{Bohr}^{sw}$. The dramatic nonlinearity of the correlation shown in Figure 10 is a result of nonidentity in Bohr entropies between the tertiary constraint and switch point transitions, whereas their identical enthalpies produce the linearity observed in Figure 9.

Table 2 summarizes the "molecular choreography" of six response functions to heme site ligation that have now been traced through all the stepwise reactions of the cascade shown in Figure 1. This tabulation illustrates the dramatic synchronization and phasing of responses that occur through specific subsets of the 16 transitions, as predicted by the symmetry rule mechanism. It may be predicted that further studies with other heterotropic effectors (e.g., organic phosphate, chloride) may also follow these same rules. The work presented from this and the previous studies on this problem have provided a framework which sets the stage for more detailed understanding of the structural and dynamic properties that underlie these correlations.

REFERENCES

Ackers, G. K. (1970) *Adv. Protein Chem. 24*, 343−446.
Ackers, G. K. (1980) *Biophys. J. 32*, 331−343.
Ackers, G. K. (1990) *Biophys. Chem. 16*, 371−382.
Ackers, G. K., & Halvorson, H. R. (1974) *Proc. Natl. Acad. Sci. U.S.A. 91*, 4312−4316.
Ackers, G. K., & Johnson, M. L. (1990) *Biophys. Chem. 37*, 265−279.
Ackers, G. K., Doyle, M. L., Myers, D., & Daugherty, M. A. (1992) *Science 255*, 54−63.
Antonini, E., Wyman, J., Brunan, M., Bucci, E., Franticelli, C., & Rossi-Fanelli, A. (1965) *J. Biol. Chem. 240*, 1096−1103.
Atha, D., Johnson, M. L., & Riggs, A. F. (1979) *J. Biol. Chem. 254*, 12390−12397.
Baldwin, J., & Chothia, C. (1979) *J. Mol. Biol. 129*, 175−220.
Blough, N. V., & Hoffman, B. M. (1984) *Biochemistry 23*, 2875−2882.
Chipperfield, J. R., Rossi-Bernardi, L., & Roughton, F. J. W. (1967) *J. Biol. Chem. 242*, 777−783.
Chu, A. H., Turner, B. W., & Ackers, G. K. (1984) *Biochemistry 23*, 604−617.
Daugherty, M. A., Shea, M. A., Johnson, J. A., LiCata, V. J., Turner, G. T., & Ackers, G. K. (1991) *Proc. Natl. Acad. Sci. U.S.A. 88*, 1110−1114.
Daugherty, M. A., Shea, M. A., & Ackers, G. K. (1994) *Biochemistry 33*, 10345−10357.
Doyle, M. L., & Ackers, G. K. (1992) *Biochemistry 31*, 11182−11195.
Doyle, M. L., Speros, P. C., LiCata, V. J., Gingrich, D., Hoffman, B. M., & Ackers, G. K. (1991) *Biochemistry 30*, 7263−7271.
Doyle, M. L., Lew, G., DeYoung, A., Kwiatkowski, L., Wierzba, A., Noble, R. W., & Ackers, G. K. (1992) *Biochemistry 31*, 8629−8639.
Edsall, J. T., & Gutfreund, H. (1983) *Biothermodynamics: A Study of Biochemical Processes at Equilibrium*, Wiley & Sons, New York.
Hill, T. L. (1960) *Introduction to Statistical Thermodynamics*, Addison-Wesley, Reading, MA.
Ip, S. H. C., & Ackers, G. K. (1977) *J. Biol. Chem. 252*, 82−87.
Johnson, J. A. (1990) Ph.D. Dissertation, The Johns Hopkins University, Baltimore, MD.
Johnson, M. L., & Frasier, S. (1985) *Methods Enzymol. 117*, 301−342.
Koshland, D. E., Nemethy, G., & Filmer, D. (1966) *Biochemistry 5*, 365−385.
LiCata, V. J., Speros, P. C., Rovida, E., & Ackers, G. K. (1990) *Biochemistry 29*, 9772−9783.
LiCata, V. J., Dalessio, P. M., & Ackers, G. K. (1993) *Proteins: Struct., Funct., Genet. 17*, 279−296.
Mills, F. C., & Ackers, G. K. (1979) *Proc. Natl. Acad. Sci. U.S.A. 76*, 273−277.
Mills, F. C., Ackers, G. K., Gaud, H., & Gill, S. J. (1979) *J. Biol. Chem. 254*, 2875−2880.
Monod, J., Wyman, J., & Changeux, J. P. (1965) *J. Mol. Biol. 12*, 88−118.
Perrella, M., Benazzi, L., Shea, M. A., & Ackers, G. K. (1990b) *Biophys. Chem. 35*, 97−103.
Rollema, H. S., deBruin, S. H., & van Os, G. A. J. (1976) *FEBS Lett. 51*, 148−150.
Silva, M. M., Rogers, P. H., & Arnone, A. (1992) *J. Biol. Chem. 25*, 17248−17256.
Smith, F. R., & Ackers, G. K. (1985) *Proc. Natl. Acad. Sci. U.S.A. 82*, 5347−5351.
Smith, F. R., & Simmons, K. C. (1994) *Proteins: Struct., Funct., Genet. 18*, 295−300.
Smith, F. R., Gingrich, D., Hoffman, B., & Ackers, G. K. (1987) *Proc. Natl. Acad. Sci. U.S.A. 84*, 7089−7093.
Speros, P. C., LiCata, V. J., Yonetani, T., & Ackers, G. K. (1991) *Biochemistry 30*, 7254−7262.
Turner, B. W. (1989) Ph.D. Dissertation, The Johns Hopkins University, Baltimore, MD.
Turner, G. J., Galacteros, F., Doyle, M. L., Turner, B. W., Pettigrew, D. W., Smith, F. R., Hedlund, B., Moo-Penn, W., & Ackers, G. K. (1992) *Proteins: Struct., Funct., Genet. 14*, 333−350.
Valdes, R., Jr., & Ackers, G. K. (1979) *Methods Enzymol. 51*, 125−141.
Williams, R. C., & Tsay, K. Y. (1973) *Anal. Biochem. 54*, 137−145.

BI942709M